J Mater Sci: Mater Med (2010) 21:2281–2286
DOI 10.1007/s10856-010-4056-y

Thermal preparation of highly porous calcium phosphate bone filler derived from marine algae

P. J. Walsh · G. M. Walker · C. A. Maggs · F. J. Buchanan

Received: 2 September 2009 / Accepted: 9 March 2010 / Published online: 24 March 2010

Abstract A sustainable marine-derived bioceramic with a unique porous structure has been developed for hard tissue repair. The conversion of alga was achieved through a novel technique, involving well controlled thermal processing followed by low pressure–temperature hydrothermal synthesis. In its preparation, a heat treatment step was required to remove the organic compounds from the algae, which reinforces the mineralised matrices. Its removal is necessary to prevent issue such as immune biocompatibility and ensure phase purity of the resultant biomaterial. This paper investigates the hydrothermal technique used for the transformation of mineralised red algae to hydroxyapatite that preserves the algae's unique structure. It specifically focuses on the effects of heat treatment on the morphology of the algae, TGA, SEM and hot stage XRD to quantity the changes.

1 Introduction

The ability to bridge bone defects still remains highly problematic and one of the biggest challenges faced in periodontal, maxillofacial, and orthopaedic surgery today [1]. One of the main issues with many newly developed synthetic based calcium phosphate (CaP) ceramics is their lack of interconnectivity between pores. For reparative cells to fulfil their functions during physiologic bone remodelling, hypoxic conditions are required to support vascularisation [2, 3]. To achieve the former, interconnecting pores are essential, as the diffusion of oxygen can only occur within a few hundred micrometers from the blood source [4]. In addition, interconnectivity will improve the degradation rate of the CaP ceramic, as a larger surface area will be in contact with physiological fluids.

Marine derived CaP ceramics offer a possible solution to this problem. Their natural interconnecting pore structure provides a diffusion network, for the calcium—proton exchange during calcification of the coral/alga [5]. It also provides a pathway to diffuse the nutrients and gases needed for growth [6]. Biocoral® and Pro-Osteon™ are two commercially available materials derived from corals. These products have pore sizes > 200 μm, which not only allows the diffusion of nutrients and gases, but also facilitates the penetration of osteoblast cells into the graft. They are fabricated from *Goniopora* and *Porites* corals, which although are not endangered, are classified as non-renewable. The Convention on International Trade in Endangered Species treaty has prohibited the harvesting of several non-renewable coral species, highlighting the need to find alternatives [7].

Mineralised red algae, in particular Corallinaceae algal offers a possible alternative source material. They have a highly porous interconnective morphology, which are rich in calcite. They are replenishable and have good aquaculture potential [8]. The potential of using algal as a bone filler was first reported by Ewers, in 1988 [9]. A perceived drawback associated with this material, is its microporosity (<10 μm) according to the literature a pore sizes > 100 μm

P. J. Walsh (✉) · F. J. Buchanan
Polymer Research Cluster, School of Mechanical and Aerospace Engineering, Queen's University of Belfast, Ashby Building, Stranmillis Road, Belfast BT9 5AH, Northern Ireland, UK
e-mail: pamelajwalsh@qub.ac.uk

G. M. Walker
School of Chemistry and Chemical Engineering, Queens University of Belfast, Belfast, Northern Ireland, UK

C. A. Maggs
School of Biological Sciences, Queens University of Belfast, Belfast, Northern Ireland, UK

are required for bone tissue repair [10]. However, two clinical studies by Schopper et al. [10] and Ewers [11], using AlgiPore (Dentsply Friadent, Mannheim, Germany) reported uniform resorption of the filler, with a 95.6% formation of new bone tissue in maxillary sinus augmentation. Ewers et al. [9] invention on the fabrication of echinoid skeletal hydroxyapatite, used a closed system hydrothermal exchange at temperature of 300–600°C, under 5–10 MPa of pressure. A novel low temperature–pressure hydrothermal synthesis, with processing temperatures < 100°C, at atmospheric pressure was reported successful in the conversion of mineralise red alga to hydroxyapatite by Walsh et al. [12]. The aim of this study is to determine the optimum processing conditions required for the conversion. The main focus of the study is the heat treatment step, which poses the greatest problem in the preparation of porous hydroxyapatite.

2 Materials and experimental procedure

2.1 Materials

Corallina officinalis a calcareous red alga, harvested from Fanad, Co. Donegal, Ireland was used for this study. Samples of seawater and alga from the collection site were tested using ICP-MS and found to be in compliances with ISO 13779-4 standard [13]. All chemicals were of reagent grade purity and purchased from Sigma–Aldrich. Distilled water was used for all experiments.

2.2 Experimental

The thermal behaviour was investigated to determine the optimum ramp rate required for the heat treatment of the algal. Thermogravimetric analysis (TGA), in air was used to investigate the effect of different ramp rates on the instantaneous reaction rate of *C. officinalis*. A commonly used empirical model for thermal decomposition of solid-state reactions was applied to the TGA data [14, 15], summarised in Eqs. 1–6. The change in mass loss, M_L with respect to time t, was related to the degree of conversion χ and the kinetic constant k, given by:

$$M_L = dM/dt = -g(\chi)k(T)\, q(\chi, T). \quad (1)$$

Additionally, $g(\chi)$ describes the degree of conversion, given by:

$$g(\chi) = (W_0 - W_f/W_\infty - W_0)^n. \quad (2)$$

And according to Arrhenius law, $k(T)$ is the function that describes the temperature dependence of the reaction rate on the temperature, given by

$$k(T) = A^{-E_A/RT} \quad (3)$$

where A is the preexponential factor, E_A is the activation energy, R is the ideal gas constant.

The maximum rate of decomposition occurred when $d^2f/dT^2 = 0$; E_A, which is expressed by

$$E_A = \eta RT^2[(dg/dT)/(1 - f_m)] \quad (4)$$

where f_m is the maximum degree of conversion.

The characteristic temperature T_0 was found at the intercept of the locus $f = 0$ (TG data) and the tangential at maximum conversion, given by:

$$T_0 = T_m - 1[(RT_m * f_m)/E_A(1 - f_m)] \quad (5)$$

The characteristic temperature T_1 was found at the intercept of the locus $f = 1$ (TG data) and the tangential at maximum conversion, given by:

$$T_1 = T_m - 1[1 + (R * T_m/E_A)] \quad (6)$$

TG Analysis was carried out using Netzsch STA 449 C Jupiter apparatus, with an air flow rate of 0.05 ml min. For this study, five different heating rates were investigated, to include: 0.5, 1, 2, 5 and 10°C min^{-1}. A mass loss study was carried out to confirm the results of the TG study. This study was carried out in an *Elite* box furnace BRF15/5, in an air atmosphere using the same heating rates.

A heat treatment study was then carried out to observe the phase transition in air, with respect to time and temperature, using the furnace. Samples were heating in temperature ranging from 400 to 800°C for a soak period of 6 and 12 h, with the optimised ramp rate. XRD was carried out on a PANalytical X'Pert PRO MPD (Model No. PW3040/60) diffractometer to determine the phase transition with respect to time and temperature. The scans were performed under CuK_α ($\lambda = 1.54$ nm) radiation and recorded in the range of $10° \leq 2\theta \leq 60°$ with a step size of 0.02° and count rate of 0.0005° min^{-1}. The results were then characterised by Rietveld refinements using Phillips X Pert High Score Software. For SEM analysis, samples were sputter coated with gold for analysis using a Fisons Instrument Coater (Polaron SC 502, UK) and analysed using a JEOL 6500 FEGSEM.

2.3 Statistical analysis

All experiments were performed in triplicate, unless otherwise specified. One-way analysis of variance (ANOVA) with a post hoc Fisher's PLSD test was applied to the mass loss data. EDX data was analyzed by one-way ANOVA with a post hoc Bonferroni test and two-way ANOVA to determine interactions between variables. A confidence level of 95% was used for all statistical analysis.

3 Results and discussion

3.1 Study of thermal kinetics

The effective removal of the organic content is fundamental and a critical component of hydrothermal synthesis. The first stage in the optimisation of ramp rate was to determine the kinetic behaviour of the algae, which was achieved using TG Analysis. Figure 1a shows the thermograms of f_m achieved under the define ramp rates. It was observed that the temperature required to achieve maximum f_m increased with respect to an increase in ramp rate in Fig. 1a, with the exception of 2°C min^{-1}. A greater f_m was required between 500 and 600°C using 2°C min^{-1}. This would suggest the sample contained a higher organic content. Overlap was observed in this ramp rate with 0.5 and 1°C min^{-1} in the temperature range of 450–600°C. Figure 1b shows the differential thermal analysis (DTA). For a reaction to take place energy is required. The main peak C was a result of the phase change from calcite to calcium oxide, producing a well defined peak. The two smaller peaks A and B correspond to the two-step reaction caused by the removal of organics. The DTA plot was used to calculate the activation energy (E_A) required to burn off organic matter. It was hypothesised that high E_A could jeopardise the stability of the alga, due to a burst effect of the organic matter with increased E_A.

Carrasco et al.'s [14] mathematical model of the thermal decomposition of green alga was used to determine the E_A. The peaks which correlate with the E_A required to burn off organics are labelled A and B in Fig. 1b. In peak A, the characteristic temperature T_0 was found at the intercept of the locus $f = 0$ and the tangential at maximum conversion in Fig. 1, which was used to determine E_A, Eq. 5. In peak B, the characteristic temperature T_1 was found at the intercept of the locus $f = 1$ and the tangential at maximum conversion in Fig. 1, which was used to determine E_A, Eq. 6.

The E_A results obtained from Fig. 1a and b for each ramp rate are reported in Table 1. It was observed that E_A increased with respect to an increase in ramp rate. Furthermore, it was found that an increase in ramp rate from 0.5 to 10°C min^{-1} resulted in an increase in E_A in the order of a magnitude of 20 for both reactions (peak A and B). The variation in E_A between ramp rates used was high for both reactions. This would suggest that the E_A was dependent on the ramp rate applied. Greater E_A was required for the second reaction (peak B), however higher temperatures were applied at this stage of conversion, which accounts for this increase.

Reina et al. [15] reported that changes in E_A were a function of the quantity of volatile matter present. However, f_m reported in Table 1 shows little variation. This would indicate that there was a relatively similar organic content in the samples used for each ramp rate. A heat study using the same ramp rates was carried to verify that the organic mass remained constant in the alga used.

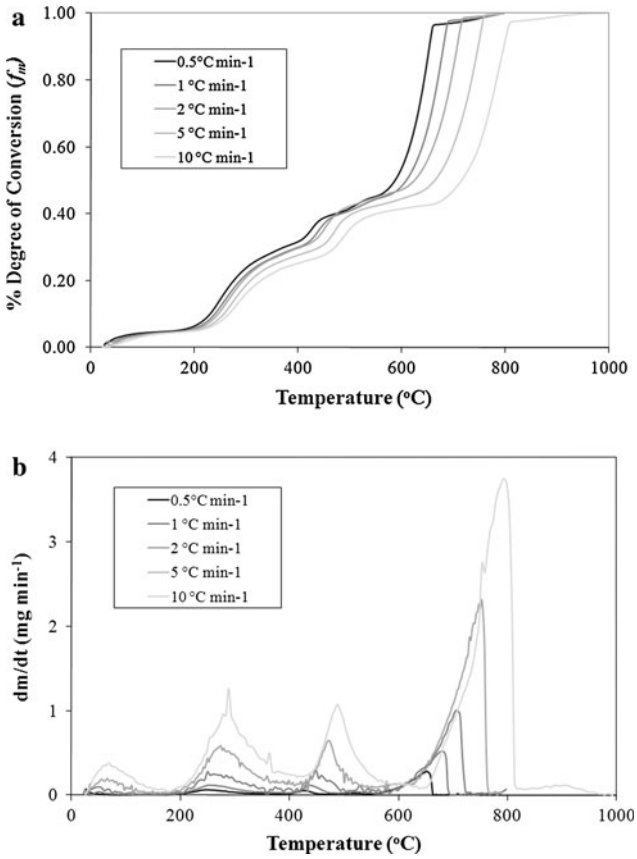

Fig. 1 **a** Degree of conversion of thermal decomposition on alga with instantaneous reaction rate using different ramp rates, under air atmosphere. **b** DTA plot of effect of temperature on instantaneous reaction rate at different ramp rates on alga, under air atmosphere (dM/dt = differential mass loss)

Figure 2 shows the results for this mass loss (M_L) study. According to Fig. 1b the complete decomposition of the organics occurred in the temperature range of 200 and 600°C. An ash temperature of 600°C was selected, to ensure that the complete decomposition of organics occurred. Furthermore, a soak time of 12 h was selected, as the ignition experiment indicated that a stable mass was achievable within this time period, reported in Walsh et al. [12] The average M_L was found to be 38.80 (±1.53) % at 600°C using different ramp rates. A high variation in M_L was observed in all ramp rates, with the exception of 0.5°C min^{-1}. However, ANOVA analysis found no significant difference ($P = 0.6841$) in M_L between ramp rates investigated. These results would indicate that the organic content was relatively constant, which suggests the variation in E_A is independent of the M_L.

Table 1 Empirical value for E_A derived from experimental data for different ramp rates applied in a TG study of *C. officinalis* alga

β (°C min^{-1})	Peak A				PeakB			
	T_m (°C)	f_m (%)	$(df/dT)_m$ (k^{-1})	E_A (kJ mol^{-1})	T_m (°C)	f_m (%)	$(df/dT)_m$ (k^{-1})	E_A (kJ mol^{-1})
0.5	263.94	14.64	0.06	174	428.17	35.80	0.06	382
1	261.32	14.79	0.12	330	440.48	35.21	0.12	784
2	254.00	11.65	0.31	811	448.14	34.83	0.29	1,930
5	279.21	14.64	0.56	1,660	473.33	35.39	0.64	4,575
10	288.03	14.08	1.26	3,840	488.03	33.11	1.08	7,777

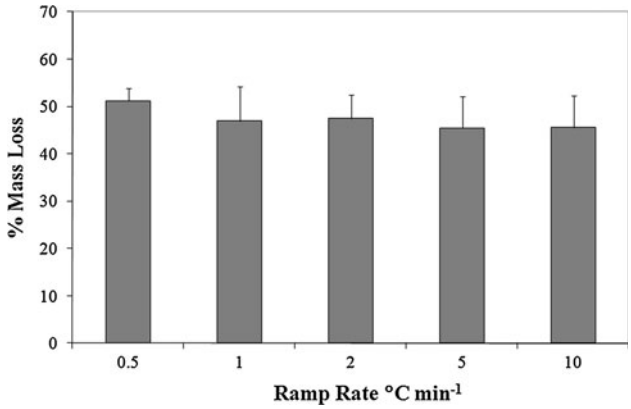

Fig. 2 M_L of alga (soak = 12 h; temperature 600°C). *Error bars* represent means standard deviation for $n = 6$

It was hypothesised that high E_A had the potential to burst the organics, jeopardising the stability of the skeletal morphology. SEM was carried out to determine the effect of different ramp rates on the morphology of the alga. Micrograph images of the raw algae were compared to heat treated algae using a ramp rate of 2 and 10°C min^{-1} are shown in Fig. 3. Organic matter was visible in the pores of the raw alga in Fig. 3a. After processing at 600°C, no organics were observed, as evident in Fig. 3b. Using a ramp rate greater than 2°C min^{-1} resulted in the partial decomposition of the original skeletal morphology. This was most pronounced using a ramp rate of 10°C min^{-1}. The resultant morphology after heating at 10°C min^{-1} is shown in Fig. 3c. From the micrograph images it was clear that cell walls have started to breakdown at 10°C min^{-1}. However, after heating at 2°C min^{-1} the honeycomb morphology that was observed in the raw material still remained intact. High E_A were observed in ramp rates of 5 and 10°C min^{-1}, suggesting that the heat energy encountered under these conditions may have damaged the morphology of the alga.

These results would suggest that the optimum ramp rate for the thermal decomposition of the algal is $\leq$2°C min^{-1}. However, grey particles were observed in alga heated with a ramp rate of 1 and 2°C min^{-1} on visual inspection, which would suggest the presence of residual carbon. Grey particles were observed in all samples heated with a ramp rate $<$ 0.5°C min^{-1}. These observations were quantified using EDX, in Fig. 4a. The results show the carbon content with respect to ramp rate, heated at 600°C for 12 h. The percentage carbon content increased from 6.01($\pm$1.98) to 10.41($\pm$2.51) % as the ramp rate increased from 0.5 to 10°C min^{-1} respectively. The average carbon content was found to be 8.38($\pm$1.85) %. All ramp rates $\geq$ 2°C min^{-1} were found to be within the range (4–8 wt%) of the carbon content found in natural HA [16]. The results showed no significant difference between the carbon content found in 1, 2 and 5°C min^{-1}, or 2 and 5°C min^{-1}, where $0.0657 \leq P \leq 0.9697$.

The maximum carbon content was observed at 400°C in Fig. 4. After 6 and 12 h soak times it was found to be 16.51($\pm$3.21) and 11.41($\pm$3.04) % respectively. From 400°C the carbon content decreases with increasing temperature after a 6 h soak period. After 12 h the same trend was observed with the exception of 600°C, where an elevated level (>12%wt) of carbon was found. At temperatures > 700°C the carbon content was found to be $\leq$7%wt. Two-way ANOVA showed no interaction between time and temperature on the carbon content in the material ($P = 0.2690$). The affect of temperature overall on the material was found to be very significant ($P = 0.0013$). The differences in carbon content over the temperature range with respect to soak time (6 and 12 h) was insignificant ($P = 0.0871$). However, when comparing the soak time at individual temperatures using one-way ANOVA a significant difference ($P = 0.0154$) in the carbon content was observed at 500°C. The trend in carbon content supports the visual observations, which showed the presence of grey material for all temperatures $<$ 600°C.

A further heat treatment study was carried out to observe the phase transition in air, with respect to time and temperature. Samples were heating in temperature ranging from 400 to 800°C for a period of 6 and 12 h. A slow ramp rate of 0.5°C min^{-1} was applied, following the outcome of the EDX results. Rietveld analysis was used to quantify the phase transition at 100°C intervals. The results obtained after 6 h heating are reported in Fig. 5a. The results have been normalised to exclude impurities, therefore it can be

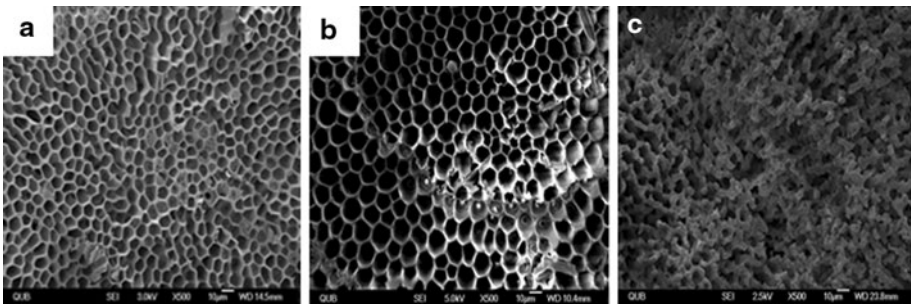

Fig. 3 Micrograph images of alga cross-section **a** raw; after heating with ramp rate of **b** 2°C min^{-1} and **c** 10°C min^{-1} (soak = 12 h; temperature 600°C)

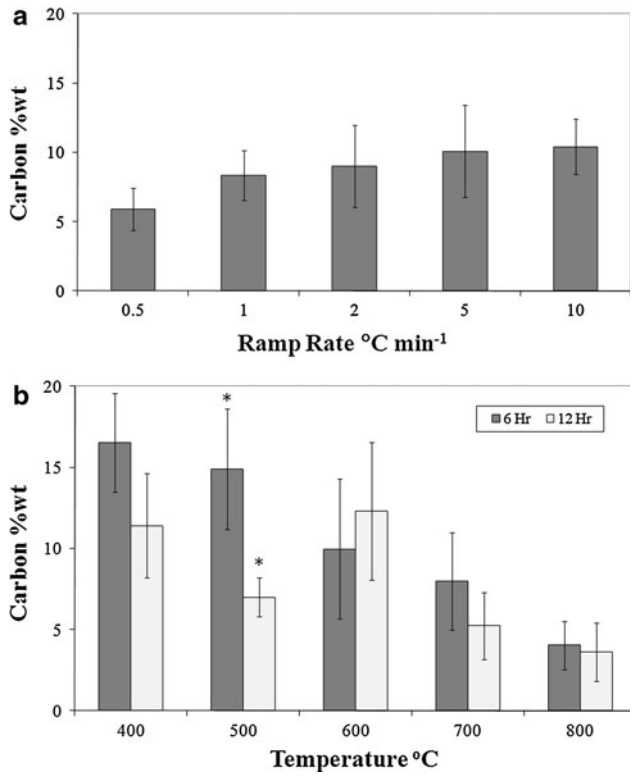

Fig. 4 **a** EDX analysis after pyrolysis at (*a*) 0.5°C min^{-1} (*b*) 1°C min^{-1} (*c*) 2°C min^{-1} (*d*) 5°C min^{-1} and (*e*) 10°C min^{-1}. **b** EDX analyses of carbon content after pyrolysis at different temperatures (ramp rate 0.5°C min^{-1}). Two-way ANOVA on temperature: degrees of freedom (d.f.) = 5.0, $P = 0.0013$; on time: d.f. = 1.0, $P = 0.0871$; * $P < 0.05$

assumed the source material is 100% Mg-rich-calcite. Little variation was observed in the chemical composition between 400 and 500°C. The calcite content remained constant at 61.40 (±0.12) %. A small decrease of 1.12% was observed in the Mg-rich-calcite. However, the presence of MgO was detected at 500°C, which supports earlier findings [12]. The dissociation of Mg from the calcite structure was more pronounced at 600°C, whereby 3.7% MgO was observed. At this temperature only a small amount of CaO (2.5%) was observed. The main phase transition to CaO was observed at 700°C, where 85.4% was observed. At this temperature 10.7% MgO was detected. A slight increase of 1.2% CaO was observed at 800°C.

The same analysis was carried out in a 12 h time period, shown in Fig. 5b. A similar trend was observed in the chemical composition after 12 h, whereby the greatest transition from $CaCO_3$ to CaO was observed at 700°C. No change was found after 12 h heating at 400°C. At 500°C a greater transition to calcite was found, 68.5% calcite was detected after 12 h as opposed to 61.4% found after 6 h at

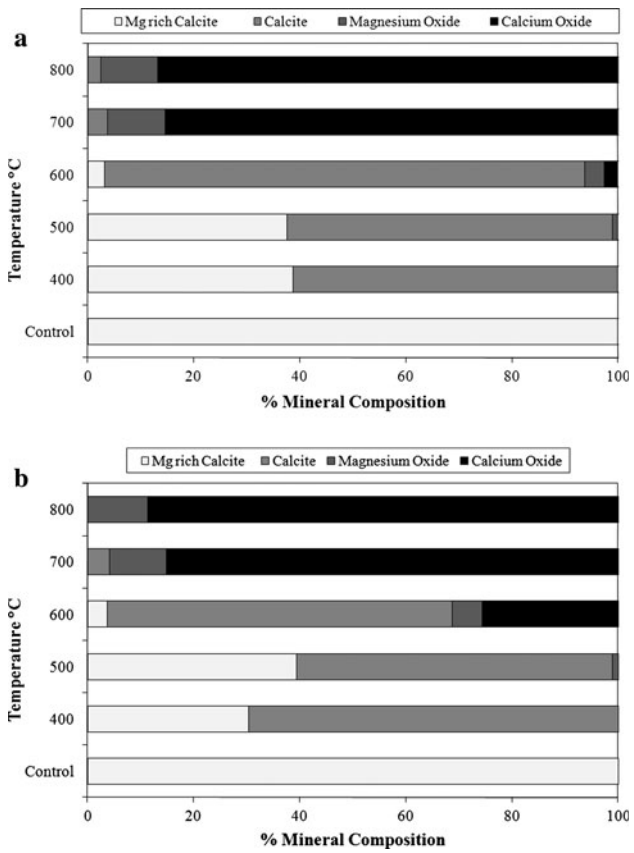

Fig. 5 **a** Rietvield date from XRD results on the phase transformation after 6 h heating with respect to temperature (ramp rate 0.5°C min^{-1}). *Note*: Normalised data to exclude impurities. **b** Rietvield data from XRD results on the phase transformation after 12 h heating with respect to temperature (ramp rate 0.5°C min^{-1}). *Note*: Normalised data to exclude impurities

the same temperature. A greater amount (25.7%) of CaO was induced at 600°C than what had previously been observed in Fig. 5a. At 700°C a similar chemical composition was observed to that after 6 h. However, after 12 h heating at 800°C no calcite was detected. These results confirmed that the chemical composition varies with respect to temperature and soak time. In both studies a greater soak time, reduced the temperature required to induce the phase transition to CaO.

The results would suggest a temperature between 600 and 700°C would be more suitable for pyrolysis with a 12 h soak period and slow ramp rate. However, Carrasco et al. [14] reported the complete destruction of the alga occurred at temperatures > 655°C. This would suggest that structure at this temperature is mechanically unstable as there is nothing to bind the mineralised phase together, indicating that the optimum processing temperature is in the range of 600 and 650°C.

4 Conclusions

Mineralised red alga was shown to be a suitable candidate for conversion to calcium phosphate ceramics in terms of its physiochemical properties. The ramp rate used during pyrolysis was found to influence the decomposition of the organic matter. The results showed that the E_A was dependent on the ramp rate applied. Furthermore, fast ramp rate, increased the E_A resulting in the decomposition of the alga's skeletal morphology. The optimum processing parameters for the thermal heat treatment were found to be in the range of 600–650°C, with a ramp rate of 2°C min^{-1}. These parameters are considered idea for hydrothermal conversion of *Corallina officinalis* to HA.

Acknowledgment This work was supported by the European Union funded STREP Project HIPPOCRATES (NMP3-CT-2003-505758).

References

1. Cancedda R, Giannoni P, Mastrogiacomo M. A review: a tissue engineering approach to bone repair in large animal models and in clinical practice. Biomaterials. 2007;28(29):4240–50.
2. Gentleman E, Swain RJ, Evans ND, Boonrungsiman S, Jell G, Ball MD, et al. Comparative materials differences revealed in engineered bone as a function of cell-specific differentiation. Nat Mater. 2009;8:763–70. doi:10.1038/NMAT2505.
3. Green DW, Bolland B, Kanczler JM, Lanham SA, Walsh D, Mann S, et al. Augmentation of skeletal tissue in impaction bone grafting using vaterite microsphere biocomposites. Biomaterials. 2009;30:1918–27.
4. Griffith LG, Naughton G. Tissue engineering—current challenges and expanding opportunities. Science. 2002;295(5557):1009–14.
5. Digby PSB. Photosynthesis and respiration in the corallina algae, clathromorphum circumscriptum and corallina officinalis and the metabolic basis of calcification. J Mar Biol Assoc. 1977;57:1111–24.
6. Karageorgiou V, Kaplan D. Poroity of 3D biomaterial scaffolds and osteogenesis. Biomaterials. 2005;26:5474–91.
7. Convention on International Trade in Endangered Species (CITES) treaty. Appendix I. [Homepage of UNEP] [Online] http://www.cites.org/. Accessed 20 Apr 2007.
8. Wilson S, Blake C, Berges JA, Maggs CA. Environmental tolerances of free-living coralline algae (maerl): implications for European marine conservation. Biol Conserv. 2004;120:279–89.
9. Ewers R, Kasperk C. Porous hydroxyl apatite material. Patent No US4770860, pp 1–4 (1988).
10. Schopper C, Moser D, Wanschitz F, Watzinger F, Lagogiannis G, Spassova E, et al. Histomorphologic findings on human bone samples six months after bone augmentation of the maxillary sinus with algipore. J Long-Term Eff Med Implants. 1999;9(3):203–13.
11. Ewers R. Maxilla sinus grafting with marine algae derived bone forming material: a clinical report of long-term results. J Oral Maxillofac Surg. 2005;63:1712–23.
12. Walsh PJ, Buchanan FJ, Bell S, Walker GM, Maggs CA, Dring MJ. Low pressure synthesis and characterisation of hydroxyapatite derived from mineralised red alga. Chem Eng. 2008;137:173–9.
13. BS ISO 13779—1:2000(E). Implants for surgery—hydroxyapatite—Part 1: ceramic hydroxyapatite. Section 4.2. Trace Elements, p 2
14. Carrasco R, Pages P. Kinetics of the thermal decomposition of green alga ulva by thermogravimetry. J Appl Polym Sci. 2004;93:1913–9.
15. Reina J, Velo E, Puigjaner L. Kinetic study of the pyrolysis of waste wood. Ind Eng Chem Res. 1998;37:4290–5.
16. Landi E, Celotti G, Logroscino G, Tampieri A. Carbonated hydroxyapatite as bone substitutes. J Eur Ceram Soc. 2003;23:2931–7.